COMPARISON OF CLOUD PROPERTIES FROM METEOSAT-8 AND SURFACE OBSERVATIONS

Patrick Minnis[(1)], Louis Nguyen[(1)], David F. Young[(1)], David R. Doelling[(2)], Michele L. Nordeen[(2)], Douglas A. Spangenberg[(2)], Rabindra Palikonda[(2)], Gregory D. Nowicki[(2)], Martial Haeffelin[(3)]

[(1)]NASA Langley Research Center, MS 420, Hampton, VA 23681 USA. Email: p.minnis@nasa.gov
[(2)]AS&M, Inc., 1 Enterprise Pkwy., Hampton, VA 23666 USA Email: d.r.doelling@larc.nasa.gov
[(3)]LMD/IPSL – Ecole Polytechnique, 91128 Palaiseau Cedex, France, Email: martial.haeffelin@lmd.polytechnique.fr

ABSTRACT

A set of algorithms used to derive cloud properties globally has been adapted to analyze hourly radiances taken by Meteosat-8. The initial results are evaluated using objective surface observations at several European locations. Cloud amounts appear to be underestimated due to the satellite retrievals missing some optically thin clouds. False cloud detections occur along arid coastlines and for heavy aerosols. Improvement in cloud detection awaits refinements of the algorithms for the SEVIRI channels and in the clear-sky radiances used to discriminate cloudy and clear scenes. Cloud-top heights are in good agreement for liquid and optically thick ice clouds but are underestimated for optically thin ice clouds. Further enhancement of the algorithms is underway.

1. INTRODUCTION

Satellite-derived cloud properties such as height, temperature, optical depth, water path, and effective particle size are important parameters for weather and icing diagnoses, estimation of surface and top of atmosphere radiation budgets, validation of climate models, and, potentially, assimilation in weather forecast models. For weather diagnoses and future data assimilations, it is necessary to have the cloud parameters available almost instantaneously in an operational mode. The capability for deriving cloud properties at high temporal resolutions has been greatly enhanced by improvements in the spectral and spatial resolutions of imagers on geostationary satellites, in particular, the Geostationary Operational Environmental Satellite (GOES) and, more recently, Meteosat-8. The new Meteosat-8 Spinning Enhanced Visible and Infrared Imager (SEVIRI) is capable of providing, at relatively high temporal and spatial resolution, the multispectral data necessary for accurate cloud retrievals. This paper describes the implementation of an analysis system to derive cloud parameters from SEVIRI data on a near-real time basis and validation of the initial products.

2. DATA & METHODOLOGY

2.1 Satellite Data and Products

Hourly 3-km SEVIRI data are acquired through the University of Wisconsin Man-computer Interactive Data Analysis System (McIDAS) in near-real time and analyzed to yield pixel-level cloud and clear-sky properties. The analysis nominally uses the radiances from the 0.64, 1.64, 3.9, 10.8, and 12.0-μm channels to classify each pixel as clear or cloudy. Cloud properties are derived using updated versions of the Visible Infrared Solar-Infrared Split-Window Technique (VISST) and Solar-Infrared Infrared Split-Window Technique (SIST) as in [1,2,3], while clear-sky spectral albedos and surface skin temperature are determined for the clear pixels. Top-of-atmosphere (TOA) shortwave albedo and outgoing longwave flux are also estimated using narrowband-broadband conversion functions. The data are processed on a 0.5° latitude-longitude grid covering the area between 30°N - 55°N and 12°W - 30°E.

Temperature and humidity profiles are interpolated to the grid and the UTC hour from 6-hourly NOAA Global Forecast System (GFS) 1.25°-resolution thinned analyses, which have 10 levels between 1000 and 100 hPa plus the surface air temperature and the tropopause height, pressure, temperature, and humidity. Sea surface temperatures are also included. Surface elevation, type, and vegetation as well as snow and ice maps at various resolutions (down to ~10 km) are also used as input. Monthly maps of surface emissivity at 3.75, 10.8, and 12.0 μm [4,5] and clear-sky albedo at overhead sun [5,6] derived for the Clouds and Earth's Radiant Energy System (CERES; Project [7] at a 10' resolution are averaged into the 0.5° grid [3].

The first step of the algorithm is to classify each imager pixel as clear or cloudy using updated versions of the pixel classification schemes described in [8]. The cloud mask for CERES nominally uses radiances taken at 0.64, 1.6, 3.7, 11 , and 12 μm. For initial application to SEVIRI data, the algorithm is modified to perform without the 1.6 μm channel. This is not a major change since the 1.6 μm channel is used

primarily in phase classification. An empirical adjustment is applied to the interpolated GFS surface air temperature to estimate skin temperature. This value is used with the surface emissivity and soundings to estimate the TOA clear-sky radiances at 3.9, 10.8, and 12.0 μm for the Meteosat-8 view at a given time and 0.5° region. Overhead-sun clear-sky albedos are used to estimate clear-sky reflectance at 0.64 μm using the inverse of the approach described by [9]. Cloud temperature T_c, top height z_{top}, thickness, effective pressure, phase, effective droplet radius r_e or effective ice crystal diameter D_e, optical depth τ, and ice *IWP* or liquid water path *LWP* are derived for each cloudy pixel using one of two methods. During daytime (solar zenith angles < 82°), the VISST is used. This is an updated version of the 3-channel daytime method described by [1] that uses the 0.65, 3.7, and 10.8 μm channels. In this initial application, the 1.6-μm channel is not used. At night, all parameters are derived using the SIST, an improved version of the 3-channel night time method described by [1]. Since only infrared channels can be used at night, SIST retrievals are valid only for optically thin clouds. For clouds with $\tau < 8$ at night, default values are used for all parameters except phase, T_c, and z_c.

2.2 Surface data

Two different types of surface datasets are used here. The first consists of surface ceilometer data taken at eight Automated Surface Observing System (ASOS) sites that are shown in white letters in Fig. 1. The second type is from the Site Instrumental de Recherche par Teledetection Atmospherique (SIRTA) at Palaiseau, France indicated in the magenta letters in Fig. 1. The complement of sensors and datasets taken at SIRTA is summarized in Table 1. The initial comparisons here only use the lidar-radar products, which can be analyzed to estimate cloud amount and base and top heights. Daytime data taken between May and August 2004 are used to evaluate the preliminary Meteosat-8 products. The SIRTA data are averaged over a 10-min interval centered on the Meteosat-8 image time. The results are compared with the VISST averages for all pixels within a 10-km radius of the

Fig. 1. Locations of surface sites

Table 1. Summary of sensors, data and availability at SIRTA.

LIDAR	*B-scat Lidar (532, 1064)*	*Clouds, aerosols properties*	*1999*
	Ceilometer (KNMI)	*Cloud, BL Height*	*2002*
	IR Doppler Lidar (10.6 μm)	3D Wind	1999
	Raman Lidar (355 nm)	Water vapor, Profile	2003
RADAR	*Doppler Radar 95 GHz*	*Cloud properties*	*2002*
	Doppler Radar 5 GHz	Precipitation, 3D Wind	1999
RADIO-METER	*BB Radiometers*	*Radiative Fluxes (2003 BSRN)*	*1999*
	Sun-Photometer	*Aerosols, water vapor*	*2002*
	MW Radiometer	*Water vapor + liquid*	*1999*
IN-SITU	*Weather*	*Pres., temp., humidity, wind*	*1999*
	Spectro-pluviometer	*Diameter + drop velocity*	*1999*
	Radiosonde	*Vertical Profiles (00, 12 UT)*	*1999*
	Sonic Anemometer	Turbulent Fluxes	2004

SIRTA site. For the cloud height comparisons, only single-layer clouds, as determined form the lidar-radar product, are evaluated for all VISST cloud amounts exceeding 80%. Ice and liquid cloud heights are examined separately using a lidar-radar cloud top altitude of 6 km to separate ice and water clouds.

The ASOS ceilometer data are used to compute cloud fraction every hour over each site in four categories: clear, scattered, broken, and overcast. The ASOS ceilometer does not report high clouds and rarely reports clear or overcast conditions. Cloud amounts are computed using all of the pixels within a 10-km radius of each ASOS site for the period between 7 and 20 August 2004. Comparisons are performed only when ASOS cloud amount is broken or overcast.

3. RESULTS

Fig. 2 shows an example of the clopud properties derived from SEVIRI data taken at 0900 UTC, 8 September 2004. The visible and infrared channels (Fig. 2a, b) show clouds over Spain and the adjacent Atlantic as well as over eastern Europe and part of the eastern Mediterranean. The cloud phase (Fig. 2c) indicates that most of the clouds are composed of liquid water. Some of the liquid clouds are supercooled (e.g., Bay of Biscay and Belarus). Ice clouds are seen over Ukraine, Algeria, Germany, Poland, and the Bay of Biscay. Areas of uncertain cloud cover (yellow areas and blocky blue) are primarily along the Italian and North African coasts. These uncertain areas as well as the area of thin clouds east of Spain have the highest values of *Tc* (Fig. 2d). Optically thin clouds (Fig. 2e) common over central Europe range in altitude from 4 - 8 km (Fig. 2f) while the thicker clouds vary from 1 km over Spain up to 12 km over Ukraine. The derived LWP (Fig. 2g) is mostly less than 100 gm^{-2}. Larger values are seen south of Ireland and north of Libya. The cloud effective pressures (Fig. 2h) track the values of z_{top}. The effective cloud droplet sizes (Fig. 2i) are generally in the typical ranges for liquid water clouds (5 - 15 μm) except for the thin clouds east of Spain and some of the clouds over Poland. In the former area, it is

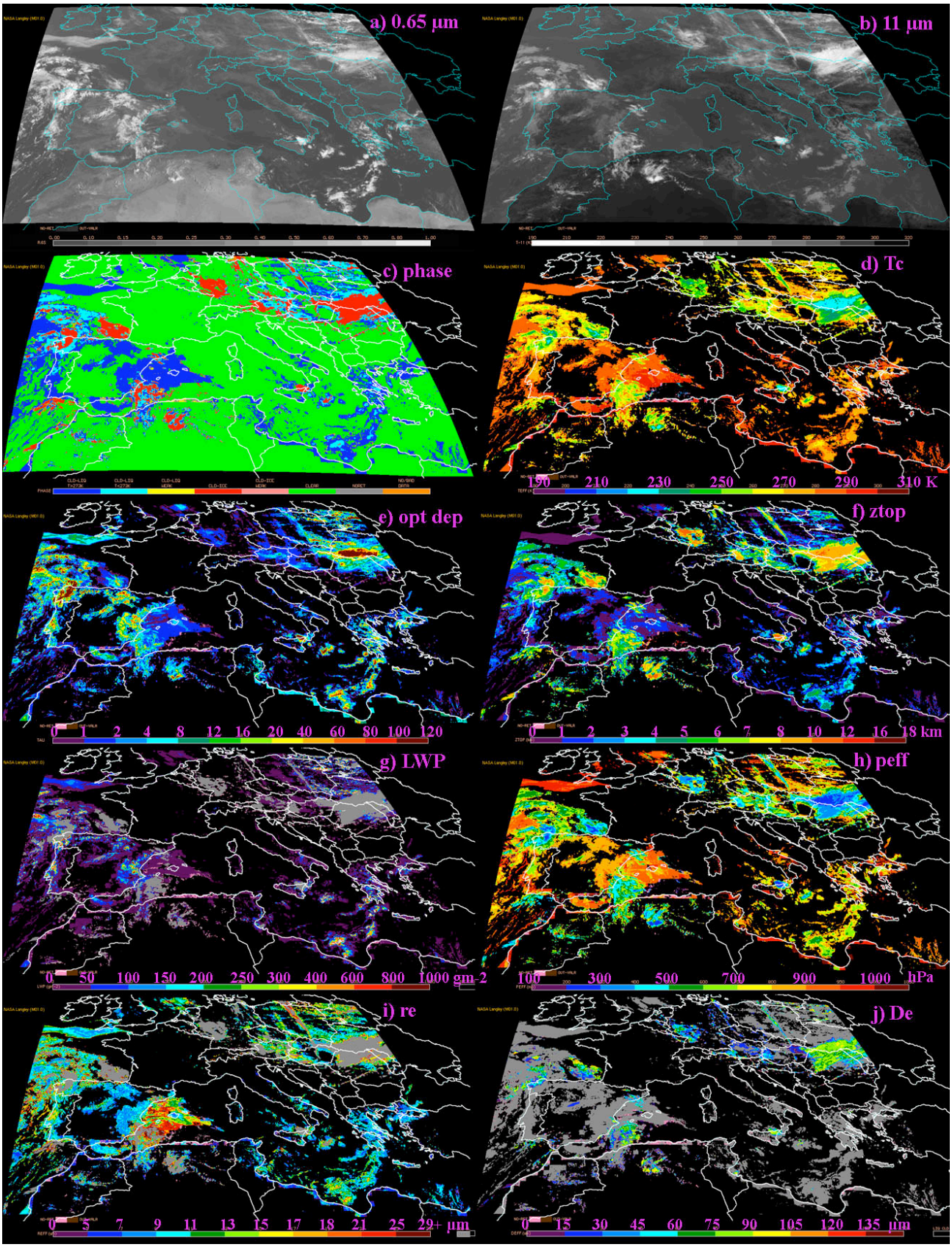

Fig. 2. SEVIRI data and derived cloud properties for 0900 UTC, 8 September 2004. (c) green denotes clear, dark and light blue are warm and supercooled liquid water clouds, red is for ice clouds, yellow is for uncertain water clouds.

Table 2. SIRTA and Meteosat-8 cloud amounts, all τ.

SIRTA	Meteosat-8			
(%)	0-20	20-50	50-80	80-100
0-20	1	0	0	0
20-50	3	0	0	7
50-80	3	0	0	9
80-100	13	5	2	55

Table 3. SIRTA and Meteosat-8 cloud amounts, τ > 5.

SIRTA	Meteosat-8 (%)			
(%)	0-20	20-50	50-80	80-100
0-20	0	0	0	0
20-50	0	0	0	11
50-80	0	0	0	7
80-100	0	2	2	79

likely that the areas where r_e > 16 μm are covered, not by clouds but by thick aerosol layer probably composed of dust from the Sahara Desert. Over Poland, high clouds over low clouds can result in the VISST retrieving water instead of ice resulting in a large effective droplet size that is unrealistic. The cloud effective ice diameters (Fig. 2j) also have values within the expected range. The largest ice crystals (D_e ~ 90 μm) are seen over Ukraine, Slovakia, and Algeria. The smallest values are evident over Germany.

Table 2 shows a comparison of the daytime cloud amounts of SIRTA for the May-August period. The lidar-radar algorithm produces very few clear cases. The surface instruments show that 75% of the time, the skies over the SIRTA site are nearly overcast and in 12% of the cases, the skies are covered by broken clouds. The SEVIRI analysis, however, finds that nearly clear skies are found in 20% of the cases. In 13% of the scenes, the lidar-radar indicated nearly overcast skies while the satellite method found less than 20% cloud cover. For the 230 cases compared here, the mean SIRTA cloud cover is 87% compared to 75% from SEVIRI. The large rms difference of 45% results from the big category differences.

If the results are restricted to clouds with τ < 5 (Table 3), then the level of agreement increases. Nearly 80% of the cases are in the near-overcast category for both methods. In most of the remaining cases, the satellite finds considerably more cloudiness than the surface instruments. On average, the SEVIRI cloud amount is 985, 8% more than from SIRTA. The rms difference drops to 24%

Table 4 shows the comparison of ASOS and Meteosat-8 cloud amounts. In general the ceilometer indicates broken or overcast conditions 86% of the time when the satellite algorithm finds the same cloud conditions.

Table 4. ASOS and Meteosat-8 cloud amounts.

Meteosat-8	All Cases	τ > 2
number	190	159
0-10%	6	1
10-50%	6	4
50-75%	4	2
75-100%	82	93

In the remaining 12% of the data, the Meteosat-8 cloud amounts are too low compared to the ceilometer. If only those clouds with τ > 2 are considered, the fraction of underestimated cloud amounts by Meteosat-8 drops to 5%.

Both the ASOS and SIRTA results suggest a number of problems with the satellite or surface algorithms, the comparison methods, or the sampling. The satellite algorithm uses a simple first guess about the clear-sky radiances. The guess for skin temperature is based on a crude conversion from the 6-hourly analyzed air temperature for a large region. The predicted 3.9-μm clear-sky temperature relies on a CERES-based value of surface emissivity, the predicted skin temperature, and a good calibration. The calibration of the 3.9-μm channel appears to have some problems [10] that have not been taken into account here. Finally, the predicted clear-sky visible reflectance depends on the CERES value. It too may be in error as evidenced by the blocky clouds along the North African coasts. Thus, the satellite algorithm needs considerable refinement.

The SIRTA algorithm may also include some aerosol layers as clouds and some very thin cirrus clouds (τ < 0.3) that are difficult to detect with most passive satellite imagers. The space and time averaging used here may not be optimal. A 10-km radius yields only about 14 pixels at the SIRTA latitude and fewer farther north and more farther south. The 10-minute advection time may be insufficient to obtain a reliable cloud amount from lidar or ceilometer data. These factors and others must be considered before drawing any conclusions about the satellite-derived cloud fractions.

A total of 51 cases met the criteria for the cloud height comparisons. Of these, 34 are for liquid clouds (Table 5). The average liquid cloud-top heights are nearly identical from the surface and satellite retrievals. The rms difference of 1.1 km is similar to other comparisons of the VISST for liquid clouds. For ice clouds, the VISST retrieval tends to underestimate the cloud-top height for optically thin clouds and to overestimate z_{top} by a smaller magnitude for thick clouds. This tendency to underestimate the height for optically thin clouds was also found by [11] and is, in part, attributable to missing some of thinnest parts of the cirrus clouds and to overestimation of the cirrus optical depth. This uncertainty can be minimized by

Table 5. SIRTA and Meteosat-8 cloud heights (km).

	Liquid	Ice ($\tau < 5$)	Ice ($\tau > 5$)
number	34	9	8
mean SIRTA	2.5	10.2	8.1
mean VISST	2.4	8.3	8.9
bias	-0.1	-1.9	0.8
rms	1.1	2.8	2.9

adjustment of the algorithms. The apparent overestimation of the thick cloud top heights is probably due to one more potential sources of error. These include the sounding used to convert *Tc* to z_{top}, and the attenuation in the radar return for very thick clouds, especially those with small ice crystals on top. These discrepancies and comparisons using multilevel and broken clouds will be examined in the future.

On average, the VISST liquid cloud thickness over SIRTA was too large by 0.4 km. The optically thick ic clouds were also too thick by 1.5 km. On the other hand, the optically thin cirrus clouds from SEVIRI were 1.3 km thinner in the mean than their SIRTA counterparts. The VISST uses a set of algorithms developed over the central United States that may not be applicable to the clouds over Europe. For the thick ice clouds, the SIRTA retrieval could be affected by the attenuation effects noted above. It is clear, however, that new parameterizations need to be developed for the Metoesat-8 domain.

5. CONCLUDING REMARKS

This paper has presented the first evaluation of the initial VISST cloud products derived from SEVIRI data over Europe and environs. A number of outstanding problems remain before the SEVIRI retrieval scan be put into an operational mode. Dust storms and some coast lines are sometimes misclassified as clouds. Distinguishing dust from clouds can be accomplished using other SEVIRI channels while the coastline misclassification can be eliminated with improved surface albedo, water percentage, and emissivity maps. Those improvements should aid the detection of optically thin clouds, which appear to be frequently missed in the cloud identification part of the retrieval process. Inclusion of calibration corrections may also help the cloud detection process and perhaps the retrieval of thin cirrus optical depths. The availability of a higher resolution meteorological analysis product would be extremely helpful for improving the retrievals.

The results are being generated every hour during daytime and will be produced at night when the daytime algorithms and input datasets have been optimized. The night time data will be analyzed using the SIST to yield improved cloud heights and thin cloud optical depths at night. The SIST employs the 3.9, 10.8, and 12.0–μm channels and will be improved using information from the 8.7 and 13.4-μm channels. Among other applications, the resulting cloud products should be valuable for interpreting broadband radiance measurements, validating forecast models, monitoring aircraft icing conditions, improving numerical weather prediction models, and understanding the diurnal cycle of atmospheric energy. The daytime results are currently being produced with a 6-hr lag and will eventually be generated in near-real time as the algorithms and input data are improved.

ACKNOWLEDGMENTS

This research was supported by the NASA Earth Science Enterprise Office, Radiation Sciences Branch.

REFERENCES

1. Minnis, P., et al. Cloud Optical Property Retrieval (Subsystem 4.3), "Clouds and the Earth's Radiant Energy System (CERES) Algorithm Theoretical Basis Document, Volume III: Cloud Analyses and Radiance Inversions (Subsystem 4)", *NASA RP 1376 Vol. 3*, edited by CERES Science Team, 135-176, 1995

2. Minnis, P., D. P. Garber, D. F. Young, R. F. Arduini, and Y. Takano, Parameterization of Reflectance and Effective Emittance for Satellite Remote Sensing of Cloud Properties, *J. Atmos. Sci.*, Vol. 55, 3313-3339, 1998.

3. Minnis, P., et al. Seasonal and Diurnal Variations of Cloud Properties Derived for CERES from VIRS and MODIS Data. *Proc. AMS 11th Conf. Atmos. Rad.*, Ogden, UT, June 3 –7, 2002.

4. Chen, Y., S. Sun-Mack, P. Minnis, D. F. Young, and W. L. Smith, Jr., Surface Spectral Emissivity Derived From MODIS Data. *Proc. SPIE 3rd Intl. Asia-Pacific Environ. Remote Sensing Symp. 2002: Remote Sens. of Atmosphere, Ocean, Environment, and Space*, Hangzhou, China, October 23-27, Vol. 4891, 361-369, 2002.

5. Minnis, P., et al. Surface and Clear-sky Albedos and Emissivities From MODIS and VIRS With Application to SEVIRI. *Proc. 2002 EUMETSAT Meteorological Satellite Conf.*, Dublin, Ireland, Sept. 2-6, 600-607, 2002.

6. Sun-Mack, S., P. Minnis, Y. Chen, and R. F. Arduini, Clear-sky Narrowband Albedos Derived from VIRS and MODIS. *SPIE 10th Intl. Symp Remote Sens., Conf. Remote Sens. Clouds and Atmos.*, Barcelona, Spain, September 8-12, 101-109, 2003.

7. Wielicki, B. A., B. R. Barkstrom, E. F. Harrison, R. B. Lee III, G. L. Smith, and J. E. Cooper, Clouds and the Earth's Radiant Energy System (CERES): An Earth Observing System Experiment. *Bull. Amer. Meteor. Soc.*, **77**, 853-868, 1996.

8. Trepte, Q., Y. Chen, S. Sun-Mack, P. Minnis, D. F. Young, B. A. Baum, and P. W. Heck, 1999: Scene identification for the CERES cloud analysis subsystem. *Proc. AMS 10th Conf. Atmos. Rad.*, Madison, WI, June 28 – July 2, 169-172.

9. Minnis, P., D. F. Young, D. R. Doelling, S. Sun-Mack, Y. Chen, and Q. Z. Trepte, Surface and Clear-sky Albedos and Emissivities from MODIS and VIRS with Application to SEVIRI. *Proc. 2002 EUMETSAT Meteorological Satellite Conf.*, Dublin, Ireland, Sept. 2-6, 600-607, 2002.

10. Doelling, D. R., L. Nguyen, and P. Minnis, Calibration Comparisons Between SEVIRI, MODIS, GOES, and AVHRR Data. *Proc. 2004 EUMETSAT Meteorological Satellite Conf.*, Prague, Czech Republic, 31 May - 4 June, 2004.

11. Mace, G. G., Y. Zhang, S. Platnick, M. D. King, P. Minnis, and P. Yang, Evaluation of Cirrus Cloud Properties From MODIS Radiances Using Cloud Properties Derived from Ground-based Data Collected at the ARM SGP Site. In press, *J. Appl. Meteorol.*, 2004.